

Beta decay of the $M_T = -1$ nucleus ^{58}Zn studied by selective laser ionization

A. Jokinen¹, M. Oinonen^{1,5}, J. Äystö¹, P. Baumann², P. Dendooven¹, F. Didierjean³, V. Fedoseyev⁴, A. Huck², Y. Jading⁵, A. Knipper², M. Koizumi⁶, U. Köster⁷, J. Lettry⁵, P.O. Lipas¹, W. Liu⁸, V. Mishin⁴, M. Ramdhane², H. Ravn⁵, E. Roeckl⁸, V. Sebastian⁹, G. Walter², the ISOLDE Collaboration⁵

¹ Department of Physics, University of Jyväskylä, FIN-40351 Jyväskylä, Finland

² Institut de Recherches Subatomiques, F-67037 Strasbourg Cedex 2, France

³ Eurisys Mesures, Strasbourg-Lingolsheim, France

⁴ Institute of Spectroscopy, Russian Academy of Sciences, 142092 Troitsk, Russia

⁵ EP Division, CERN, CH-1211 Genève 23, Switzerland

⁶ Japan Atomic Energy Research Institute, 1233 Watanuki, Takasaki, Gunma 370-12, Japan

⁷ Physik-Department, Technische Universität München, D-85748 Garching, Bavaria

⁸ Gesellschaft für Schwerionenforschung, D-64220 Darmstadt, Germany

⁹ Institut für Physik, Johannes Gutenberg-Universität, D-55099 Mainz, Germany

Received: 5 June 1998 / Revised version: 24 July 1998

Communicated by D. Guereau

Abstract. Beta decay of ^{58}Zn has been studied for the first time. A new laser ion-source concept has been used to produce mass-separated sources for beta and gamma spectroscopy. The half-life of ^{58}Zn was determined to be 86(18) ms. Comparisons are made with previous data from charge-exchange reactions. Our Gamow–Teller strength to the 1^+ state at 1051 keV excitation in ^{58}Cu agrees well with the value extracted from a recent ($^3\text{He}, t$) study. Extensive shell-model calculations are presented.

PACS. 27.40.+z $39 \leq A \leq 58$ – 29.25.Rm Radioactive ion sources – 32.80.Rm Multiphoton ionization – 21.10.Hw Spin, parity and isobaric spin – 21.60.Cs Shell model

1 Introduction

The study of beta decay provides a direct method to obtain information on the Gamow–Teller (GT) strength, but it carries the limitation set by the Q value. For this reason, charge-exchange reactions have often been applied to extract GT strengths over a wider energy range. In particular, the cross section of a charge-exchange reaction at small angles and intermediate energies yields the GT transition strength [1]. However, this method has not been tested widely enough in view of its importance to understanding the fundamental problems of GT quenching and solar neutrinos [2,3]. It is to be noted that so far charge-exchange reactions have only been performed on stable target nuclei.

Various charge-exchange reactions on ^{58}Ni at intermediate energies have been studied in great detail. They include $^{58}\text{Ni}(p, n)^{58}\text{Cu}$ [4], $^{58}\text{Ni}(^3\text{He}, t)^{58}\text{Cu}$ [5,6] and $^{58}\text{Ni}(^6\text{Li}, ^6\text{He})^{58}\text{Cu}$ [7]. The lower-lying region of the same states in ^{58}Cu can be reached via beta decay of ^{58}Zn . Thus it is possible to obtain a direct comparison between charge-exchange reactions and beta decay.

Taking into account that ^{58}Zn is not very far from stability and that the decays of ^{57}Zn [8] and ^{59}Zn [9,10] are known, it is surprising that so little is known about the beta decay of ^{58}Zn . Seth et al. have measured its mass with an accuracy of 50 keV/ c^2 with the double-charge-exchange reaction $^{58}\text{Ni}(\pi^+, \pi^-)^{58}\text{Zn}$ [11] leading to $Q_{\text{EC}} = 9370(50)$ keV for ^{58}Zn [12]. The half-life of ^{58}Zn beta decay has not been measured so far, but Honkanen et al. [13] have reported a short-lived delayed-proton activity which agrees with the half-life limits of 50–80 ms set by the predictions [14].

2 Experimental method

The present study was performed at the ISOLDE on-line separator facility at CERN [15]. Isotopes of interest were produced in spallation reactions on Nb induced by a pulsed 1 GeV proton beam from the PS/Booster with an average beam intensity of 2.8 μA . The effective target thickness was about 48 g/cm². The target was heated to 2000–2100°C to speed up the release of Zn isotopes from it. A chemically selective laser ion source (LIS) was employed to obtain a pure ^{58}Zn beam in spite of the much

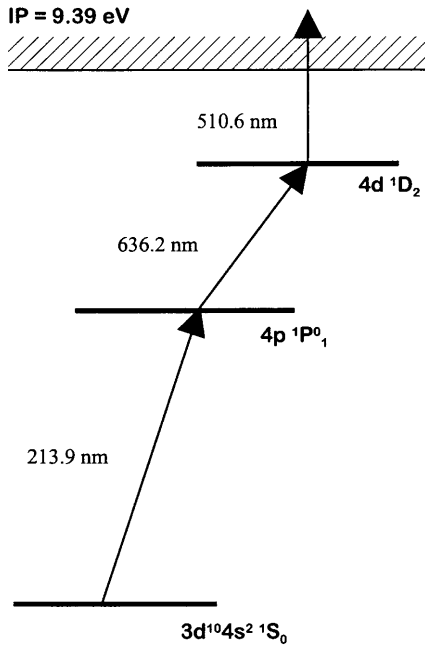


Fig. 1. New ionization scheme for Zn, used for the first time in this experiment to enhance the yield of Zn over the copiously produced isobaric contaminants. The strong UV-laser beam needed for the first resonant step of Zn is achieved via frequency tripling of the dye-laser light [32]

larger production cross sections of isobaric contaminants such as ^{58}Cu and ^{58}Mn . These two were observed during the experiment, but with much lower yields than expected for a conventional surface ionizer. More details of the new LIS scheme for Zn can be found in Ref. [16].

The Zn beam was implanted into a movable aluminized mylar tape surrounded by a detector setup. The latter consisted of a large (70%) high-purity Ge detector for gamma rays, a beta telescope and a novel charged-particle detector employing a gas ΔE detector and a Si detector [17]. The data were stored in list mode with each event tagged with the time from the last proton pulse hitting the target and with time marks of each parameter counted from the master trigger. In addition, singles spectra were accumulated in multispectrum mode.

A large fraction of the beam time was devoted to tests of the target and ion source, and to tuning the new laser ionization scheme shown in Fig. 1. The efficiency of laser ionizing stable Zn isotopes was measured to be about 5%. Release-time measurements for the target and the ion source showed a fast release of Zn with typical release parameters $\tau_r = 120 \text{ ms}$, $\tau_f = 500 \text{ ms}$, $\tau_s = 13 \text{ s}$ and $a = 0.74$ in the notation of Lettry et al. [18]. These values correspond to a release fraction of 0.5% for a half-life of 65 ms.

The main $A = 58$ contaminant is ^{58}Mn . This is because its production rate is very high in spallation of Nb and because Mn is easier to surface-ionize than Zn. In addition, the vapour pressure of Mn is high compared to Cu at the operating temperatures of the target and ion source. With the LIS the amount of ^{58}Cu contamination was negligible and the amount of ^{58}Mn was considerably

Table 1. Production rates of ^{58}Zn , ^{58}Cu and ^{58}Mn in a hot-plasma ion source and our laser ion source coupled to a Nb-foil target. For the plasma ion source, the Zn and Cu data are extrapolated from heavier isotopes

Nucleus	Production rate [ions/s]	
	Hot plasma	LIS
^{58}Zn	2	8
^{58}Cu	6×10^3	<8
^{58}Mn	7×10^5	4×10^4

reduced, although it was still as high as 4×10^4 ions/s. This number is much higher than the production rate of Zn, 8 ions/s. Fortunately it was possible to increase the ratio of ^{58}Zn activity to ^{58}Mn activity by making use of the large difference between their half-lives [$T_{1/2}(^{58}\text{Mn}) = 65.3 \text{ s}$]. In Table 1, the yields of Mn, Cu and Zn isotopes from a plasma ion source and the laser ion source show enhancement factors of ≈ 3000 and 70 for the ratios Zn/Cu and Zn/Mn, respectively.

3 Results

The nucleus ^{58}Cu is unusual in that the $T = 1$, $J^\pi = 0^+$ isobaric analogue state (IAS) lies only 203 keV above the $T = 0$, $J^\pi = 1^+$ ground state. The strong gamma transition between these states enabled us to measure the half-life of the beta decay of ^{58}Zn . The time behaviour of the beta-gated 203 keV gamma transition is presented in Fig. 2. The half-life was fitted by assuming one-component decay and no background. This first measurement of the half-life of the beta decay of ^{58}Zn gave 86(18) ms, in good agreement with the value of 50–80 ms expected from systematics [14] and with the observation of Honkanen et al. [13].

Because of the low yield of ^{58}Zn and the large fraction of beta feeding due to the Fermi transition to the IAS, we could observe only one additional beta branch, namely the GT transition to an excited state at 1051 keV. This GT transition was identified by observing an 848 keV gamma transition de-exciting the 1051 keV level. From the intensity ratio of the 203 and 848 keV gamma transitions we found the feeding ratio to the states at 1051 and 203 keV. The beta-gated gamma spectrum is shown in Fig. 3. No beta-delayed proton decay was observed, which sets an upper limit of 3% on this decay branch.

To extract the beta strength we have used the formula

$$ft = \frac{C}{B(F) + B(GT)}. \quad (1)$$

The reduced transition probabilities are related to the standard squared Fermi and Gamow–Teller matrix elements [19] according to

$$B(F) = \langle M_F \rangle^2, \quad B(GT) = (g_A/g_V)^2 \langle M_{GT} \rangle^2. \quad (2)$$

For the constants we use $C = 6145(4) \text{ s}$ [20] and $|g_A/g_V| = 1.266(4)$ [21].

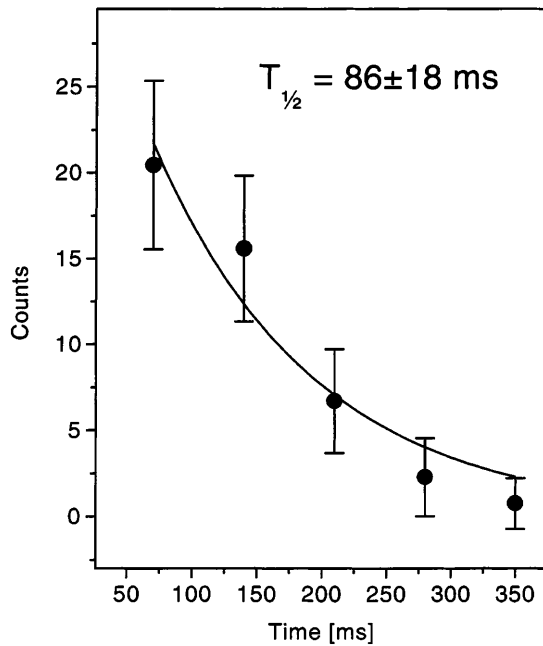


Fig. 2. Intensity of the beta-gated 203 keV gamma transition, measured as a function of the time elapsed after closing the beam gate. One-component fitting resulted in a half-life of 86(18) ms

The partial half-life t to the excited state at 1051 keV was deduced as follows. The transition to the IAS is of pure Fermi character with $B(F) = 2$, whence $\log ft = 3.48$. With this value and Eq. (1) we get, from $Q_{EC} = 9370(50)$ keV [12] and $T_{1/2} = 86(18)$ ms, a 74(16)% feeding to the 203 keV state. The experimental ratio of the beta feeding to the 1051 and 203 keV levels was deduced

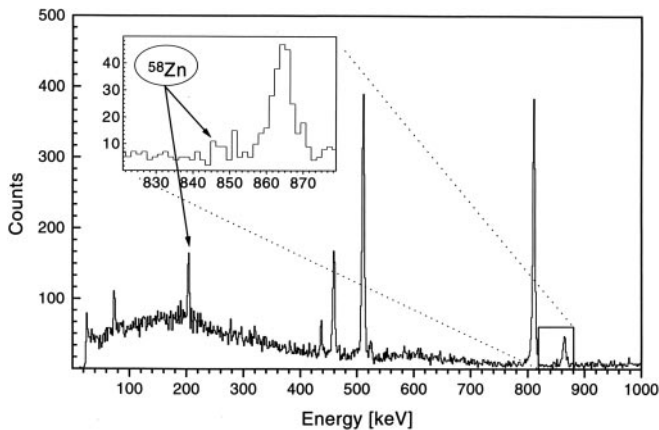


Fig. 3. Gamma spectrum obtained in coincidence with beta decay in time interval 20–450 ms from the preceding proton pulse. The beta window was restricted to energies >800 keV to enhance the intensity of gamma transitions following beta decay of ^{58}Zn . In addition to the 203 keV line originating from the beta decay of ^{58}Zn one can observe only gamma transitions from the beta decay of ^{58}Mn . The insert shows an enlargement of the spectrum in the region where the 848 keV transition was observed

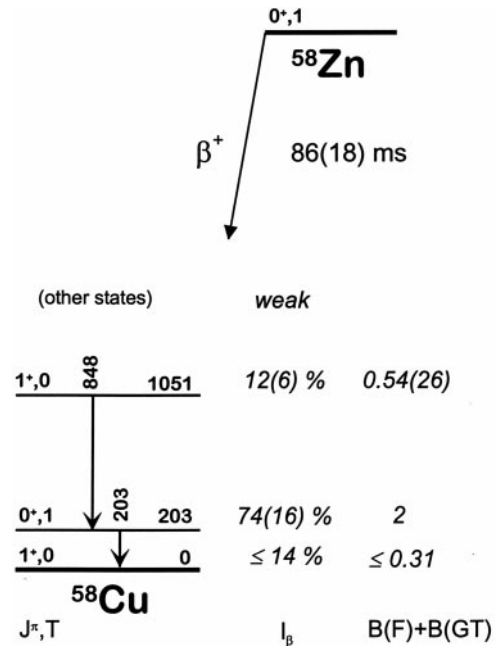


Fig. 4. Decay scheme of ^{58}Zn as obtained in this study

from the measured intensities of the 848 and 203 keV gamma transitions. This ratio and the above beta feeding of the IAS result in a 12(6)% beta feeding to the 1051 keV state. The corresponding GT strength from Eq. (1) is $B(GT; 1051) = 0.54(26)$. We may assume that the remaining 14(17)% of the beta intensity feeds the ground state, which gives $\log ft \gtrsim 4.3$ or $B(GT) \lesssim 0.31$. The partial decay scheme of ^{58}Zn is shown in Fig. 4.

4 Shell-model calculations

We undertook a series of shell-model calculations with the code OXBASH [22] applied to recent numerical Hamiltonians [23,24] fitted to the fp shell. Previous shell-model calculations on the relevant $A = 58$ nuclei have been reported by Rapaport et al. [4] and Fujita et al. [5] in connection with their studies of charge-exchange reactions. The latter theoretical results draw on large-scale calculations by Nakada et al. [25]. All calculations are carried out in the isospin formalism.

Our shell-model space is based on an inert $^{40}_{20}\text{Ca}_{20}$ core and it includes the orbitals $1f_{7/2}$, $2p_{3/2}$, $1f_{5/2}$ and $2p_{1/2}$. The previous calculations have used the same orbitals, with their occupation structured for the present case ($^{58}_{28}\text{Ni}_{30}$, $^{58}_{29}\text{Cu}_{29}$, $^{58}_{30}\text{Zn}_{28}$) as

$$(1f_{7/2})^{16-k}(2p_{3/2}, 1f_{5/2}, 2p_{1/2})^{2+k}. \quad (3)$$

Rapaport et al. include all configurations with $k = 0$ and 1, while Nakada et al. extend their space to $k = 2$.

We performed preliminary calculations with the Hamiltonian of van der Merwe et al. [24] explicitly tailored to $k = 0$ and 1. The excitation spectrum of ^{58}Ni was well reproduced, but that of ^{58}Cu was much too compressed.

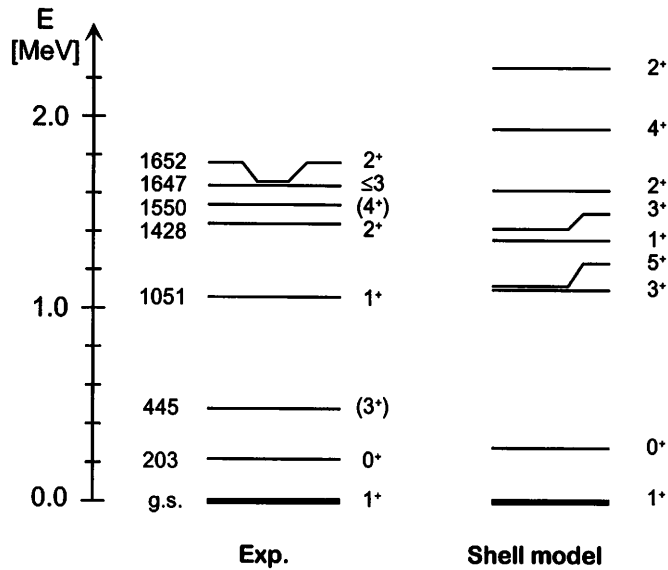


Fig. 5. Experimental [33] and calculated excitation energies of low-lying levels in ^{58}Cu

Our main shell-model calculations used the full-fp-space Hamiltonian FPD6 of Richter et al. [23]. After trial calculations with $k = 0, 1, 2$, we opted for a truncation scheme we believe to be more consistent. This truncation scheme, due to Horoi et al. [26], is based on early work by French and Ratcliff [27]. In it, an m -scheme average energy is calculated for each configuration, and all configurations up to a user-chosen cutoff energy are included.

In our work the cutoff excitation energy was 21.2 MeV. This produced a list of 30 configurations, which included most $k = 2$ and two $k = 3$ configurations. The resulting JT matrix dimensions were only a few thousands, but convergence problems appeared with a higher cutoff. The excitation energies were well reproduced; see Fig. 5. We also checked the $3(N - Z)$ sum rule [28] for GT transitions from ^{58}Zn , with the result that 91% of the sum rule is carried by the final states included in the space.

5 Discussion

Beta decay of ^{58}Zn provides an excellent test of the validity of charge-exchange reactions as a probe of GT strength in medium-heavy nuclei. Beta-decay half-lives deduced from GT strengths observed in charge-exchange reactions are listed in Table 2 and can be compared with the measured beta-decay half-life of 86(18) ms. The agreement is good between the reaction and decay studies, as expected from the Fermi dominance.

Table 2 also shows our shell-model results for comparison. The well-known global trend is that the shell-model overestimates GT strength by nearly a factor of two. This is indeed the case for the GT transition to the 1051 keV level, whereas for the ground-state transition the shell-model prediction is a factor of two too *small*. Figure 6 shows our shell-model prediction up to 16 MeV excitation

Table 2. Gamow–Teller strengths to low-lying states in ^{58}Cu and half-life for ^{58}Zn beta decay from various sources: $^{58}\text{Ni}(p, n)^{58}\text{Cu}$ [4], $^{58}\text{Ni}(^3\text{He}, t)^{58}\text{Cu}$ [5], the present experiment and our shell-model calculations (SM). For charge-exchange reactions $B(\text{GT}; \text{g.s.})$ is taken from the ground-state beta decay of ^{58}Cu [31]. The half-lives from charge-exchange data were evaluated from the $B(\text{GT})$ values by using $Q_{\text{EC}} = 9370(50)$ keV [12]

Source	$B(\text{GT}; \text{g.s.})$	$B(\text{GT}; 1051)$	$T_{1/2}$ [ms]
(p, n)	0.264(6)	0.72(14)	82
($^3\text{He}, t$)	0.264(6)	0.46(10)	86
$^{58}\text{Zn}(\beta^+)$	$\lesssim 0.31$	0.54(26)	86(18)
SM	0.144	1.122	

in ^{58}Cu , with the (p, n) data [4] displayed for comparison; only the two lowest states are seen in beta decay. In spite of the differences in detail, the cumulative strengths roughly parallel each other up to some 12 MeV. This is seen in Fig. 7, which shows the cumulative GT strengths from the experiment [4] and the shell model. Only in the high-energy region does the shell model display the expected overestimation.

The population of the first excited 1^+ state in ^{58}Cu at 1051 keV agrees well with the results from charge-exchange reactions, particularly ($^3\text{He}, t$), as seen from Table 2. The fact that the $B(\text{GT})$ value for the 1051 keV state from the (p, n) study is somewhat higher than those from beta decay and ($^3\text{He}, t$) may be due to differences in resolution. The relatively poor resolution of the (p, n) study makes it difficult to extract individual strengths for the 1^+ ground state, the IAS at 203 keV and the 1^+ state at 1051 keV.

It is known from an old ($^3\text{He}, t$) reaction study [29] that the transition to the excited state at 1051 keV involves $l = 2$ transfer, which is required to explain the measured angular distribution of tritons. Nevertheless the recent ($^3\text{He}, t$) study at intermediate energies (150 MeV/u)

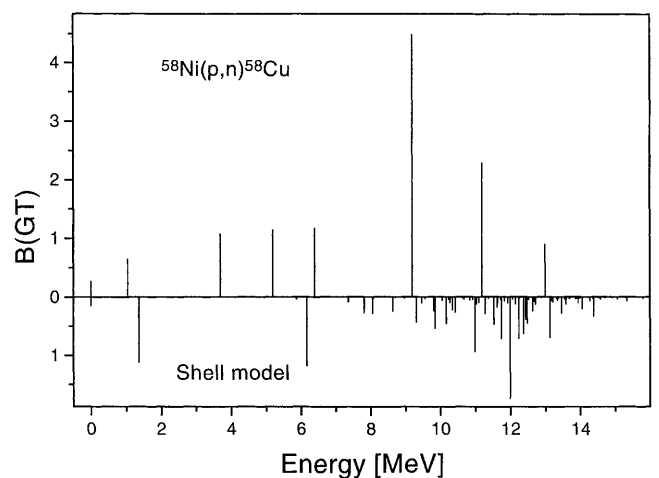


Fig. 6. Gamow–Teller strength for ^{58}Cu final states from the (p, n) reaction [4] and our shell model

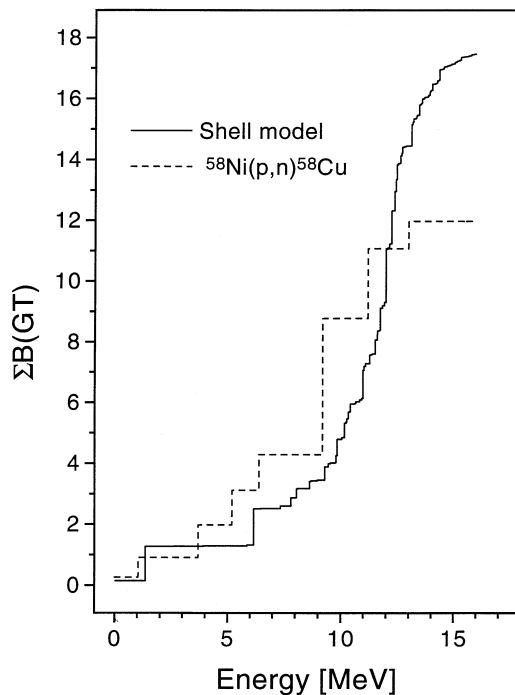


Fig. 7. Cumulative Gamow-Teller strength from the (p, n) reaction [4] and our shell model

[5] compares well to our results, suggesting that this reaction at these bombarding energies provides an appropriate choice for extracting GT strength. Contrariwise, a major difference was obtained for l -forbidden transitions when comparing GT strength extracted from beta decay of ^{38}Ca and the reaction $^{38}\text{Ar}(p, n)^{38}\text{K}$ [2]. It was possible to describe the difference by means of an empirical (p, n) operator. This operator was first introduced to explain cases where (p, n) GT strength was enhanced relative to beta decay [30].

The non-observation of protons in the present study corresponds to an upper limit of 3% on a beta-delayed proton branch. This value agrees well with the 2.4% we deduce from the (p, n) GT strength [4] above the proton binding energy and inside the beta-decay window. A future observation of protons would be of interest for information on higher-lying GT strength. This is particularly important because at higher ^{58}Cu excitation energies the extraction of GT strength from charge-exchange reactions involves subtraction of background due to higher l values. This background increases with an increasing excitation energy, which makes its subtraction delicate.

Finally, it would be important to redetermine the fraction of ^{58}Cu beta decays to the ^{58}Ni ground state. The strength of this transition, so far measured in only one experiment [31], is used for the calibration of $B(\text{GT})$ values from the $^{58}\text{Ni}(p, n)$ and $^{58}\text{Ni}(^3\text{He}, t)$ reactions.

This work was supported in part by GSI Darmstadt, IN2P3 (Institut National de Physique Nucléaire et de Physique Particules) and the Academy of Finland. W.L. wishes to thank Deutscher Akademischer Austauschdienst and the

Hongkong Qiushi Science Foundation for support. We are grateful to Yoshitaka Fujita for making his unpublished data available to us.

References

1. C.D. Goodman, C.A. Goulding, M.B. Greenfield, J. Rapaport, D.E. Bainum, C.C. Foster, W.G. Love, F. Petrovich, *Phys. Rev. Lett.* **44**, 1755 (1980)
2. B.D. Andersson, A.R. Baldwin, P. Baumann, B.A. Brown, F. Didierjean, C.G. Foster, L.A.C. Garcia, A. Huck, A. Knipper, R. Madey, D.M. Manley, G. Marguier, M. Ramdhane, H. Ravn, C. Richard-Serre, G. Walter, J. Watson, *Phys. Rev. C* **54**, 602 (1996)
3. W. Trinder, E.G. Adelberger, B.A. Brown, Z. Janas, H. Keller, K. Krumbholz, V. Kunze, P. Magnus, F. Meissner, A. Piechaczek, M. Pfutzner, E. Roeckl, K. Rykaczewski, W.-D. Schmidt-Ott, M. Weber, *Nucl. Phys. A* **620**, 191 (1997), and references therein
4. J. Rapaport, T. Taddeucci, T.P. Welch, C. Gaarde, J. Larsen, D.J. Horen, E. Sugarbaker, P. Koncz, C.C. Foster, C.D. Goodman, C.A. Goulding, T. Masterson, *Nucl. Phys. A* **410**, 371 (1983); J. Rapaport, T. Taddeucci, T.P. Welch, D.J. Horen, J.B. McGrory, C. Gaarde, J. Larsen, E. Sugarbaker, P. Koncz, C.C. Foster, C.D. Goodman, C.A. Goulding, T. Masterson, *Phys. Lett. B* **119**, 61 (1982)
5. Y. Fujita, H. Akimune, I. Daito, M. Fujiwara, M.N. Harakeh, T. Inomata, J. Jänecke, K. Katori, H. Nakada, S. Nakayama, A. Tamii, M. Tanaka, H. Toyokawa, M. Yosoi, *Phys. Lett. B* **365**, 29 (1996); Y. Fujita (private communication)
6. H. Akimune, I. Daito, Y. Fujita, M. Fujiwara, M.B. Greenfield, M.N. Harakeh, T. Inomata, J. Jänecke, K. Katori, S. Nakayama, H. Sakai, Y. Sakemi, M. Tanaka, M. Yosoi, *Nucl. Phys. A* **569**, 245c (1994)
7. H. Laurent, S. Gales, D. Beaumel, G.M. Crawley, J.E. Finck, S. Fortier, J.M. Maison, C.P. Massolo, D.J. Mercer, J.S. Winfield, G.H. Yoo, *Nucl. Phys. A* **569**, 297c (1994)
8. D.J. Vieira, D.F. Sherman, M.S. Zisman, R.A. Gough, J. Cerny, *Phys. Lett. B* **60**, 261 (1976)
9. J. Honkanen, M. Kortelahti, K. Eskola, K. Vierinen, *Nucl. Phys. A* **366**, 109 (1981)
10. Y. Arai, E. Tanaka, H. Miyatake, M. Yoshii, T. Ishimatsu, T. Shinozuka, M. Fujioka, *Nucl. Phys. A* **420**, 193 (1984)
11. K.K. Seth, S. Iversen, M. Kaletka, D. Barlow, A. Saha, R. Soundranayagam, *Phys. Lett. B* **173**, 397 (1986)
12. G. Audi, O. Bersillon, J. Blachot, A.H. Wapstra, *Nucl. Phys. A* **624**, 1 (1997)
13. J. Honkanen, M.D. Cable, R.F. Parry, S.H. Zhou, Z.Y. Zhou, J. Cerny, *Bull. Am. Phys. Soc.* **28**, 714 (1983)
14. J. Hardy, AECL-5032, 1975 (unpublished)
15. E. Kugler, D. Fiander, B. Jonsson, H. Hass, A. Przewloka, H.L. Ravn, D.J. Simon, K. Zimmer, ISOLDE Collaboration, *Nucl. Instr. Meth. B* **70**, 27 (1992)
16. J. Lettry, R. Catherall, V. Fedoseyev, G.J. Focker, G. Huber, O.C. Jonsson, E. Kugler, M. Koizumi, U. Köster, V.I. Mishin, H.L. Ravn, V. Sebastian, C. Tamburella, ISOLDE Collaboration, *Rev. Sci. Instr.* **69**, 762 (1998)
17. A. Honkanen, M. Oinonen, K. Eskola, A. Jokinen, J. Äystö, ISOLDE Collaboration, *Nucl. Instr. Meth. A* **395**, 217 (1997)

18. J. Lettry, R. Catherall, P. Drumm, P. Van Duppen, A.H.M. Evensen, G.J. Focker, A. Jokinen, O.C. Jonsson, E. Kugler, H. Ravn, ISOLDE Collaboration, Nucl. Instr. Meth. B **126**, 130 (1997)
19. P.J. Brussaard, P.W.M. Glaudemans, *Shell-Model Applications in Nuclear Spectroscopy* (North-Holland, Amsterdam 1977), Ch. 12
20. I. Towner, E. Hagberg, J.C. Hardy, V.T. Koslowsky, G. Savard, in *Int. Conf. on Exotic Nuclei and Atomic Masses, ENAM 95, Arles, 1995*, edited by M. de Saint Simon, O. Sorlin (Editions Frontières, Gif-sur-Yvette 1995), p. 711
21. K. Schreckenbach, P. Liaud, R. Kossakowski, H. Nastoll, A. Bussiere, J.P. Guillaud, Phys. Lett. B **349**, 427 (1995)
22. B.A. Brown, A. Etchegoyen, W.D.M. Rae, MSU-NSCL 524, 1988 (unpublished)
23. W.A. Richter, M.G. van der Merwe, R.E. Julies, B.A. Brown, Nucl. Phys. A **523**, 325 (1991); **577**, 585 (1994)
24. M.G. van der Merwe, W.A. Richter, B.A. Brown, Nucl. Phys. A **579**, 173 (1994)
25. H. Nakada, T. Sebe, T. Otsuka, Nucl. Phys. A **571**, 467 (1994)
26. M. Horoi, B.A. Brown, V. Zelevinsky, Phys. Rev. C **50**, R2274 (1994)
27. J.B. French, K.F. Ratcliff, Phys. Rev. C **3**, 94 (1971)
28. C. Gaarde, J.S. Larsen, M.N. Harakeh, S.Y. van der Werf, M. Igarashi, A. Müller-Arnke, Nucl. Phys. A **334**, 248 (1980)
29. H. Rudolph, R.L. McGrath, Phys. Rev. C **8**, 247 (1973)
30. J.W. Watson, W. Pairsuwan, B.D. Anderson, A.R. Baldwin, B.S. Flanders, R. Madey, R.J. McCarthy, B.A. Brown, B.H. Wildenthal, C.C. Foster, Phys. Rev. Lett. **55**, 1369 (1985)
31. H. Jongsma, A.G. Da Silva, J. Bron, H. Verheul, Nucl. Phys. A **179**, 554 (1972)
32. V. Fedoseyev, V.I. Mishin, Opt. Comm. (to be published)
33. L.K. Peker, J. Nucl. Data **61**, 189 (1990)